Published in final edited form as:
Cytometry A. 2009 June ; 75(6): 510–519. doi:10.1002/cyto.a.20727.

Induction of DNA Damage Response by the Supravital Probes of Nucleic Acids

Hong Zhao[1], **Frank Traganos**[1], **Jurek Dobrucki**[2], **Donald Wlodkowic**[3,4], and **Zbigniew Darzynkiewicz**[1]

[1]Brander Cancer Research Institute, and Department of Pathology, New York Medical College, Valhalla, NY, USA [2]Division of Cell Biophysics, Faculty of Biochemistry, Biophysics and Biotechnology, Jagiellonian University, Krakow, Poland [3]Department of Biological Sciences, Glasgow Caledonian University, Glasgow, UK [4]Cytotech Consultancy, Edinburgh, UK

Abstract

The aim of this study was to assess the potential DNA damage response (DDR) to four supravitally used biomarkers Hoechst 33342 (Ho 42), DRAQ5, DyeCycle Violet (DCV) and SYTO 17. A549 cells were exposed to these biomarkers at concentrations generally applied to live cells and their effect on histone H2AX (Ser 139), p53 (Ser15), ATM (Ser1981) and Chk2 (Thr68) phosphorylation was assessed using phospho-specific Abs. Short-term treatment with Ho 42 led to modest degree of ATM activation with no evidence of H2AX, Chk2 or p53 phosphorylation. However, pronounced ATM, Chk2 and p53 phosphorylation and perturbed G_2 progression were seen after 18 h. While short-term treatment with DRAQ5 induced ATM activation with no effect on H2AX, Chk2 and p53, dramatic changes marked by a high degree of H2AX, ATM, Chk2 and p53 phosphorylation, all occurring predominantly in S phase cells, and a block in cell cycle progression, were seen after 18 h exposure. These changes suggest that the DRAQ5-induced DNA lesions may become converted into double-strand DNA breaks during replication. Exposure to DCV also led to an increase in the level of activated ATM and Chk2 as well as of phosphorylated p53 and accumulation of cells in G_2M and S phase. Exposure to SYTO 17 had no significant effect on any of the measured parameters. The data indicate that supravital use of Ho 42, DRAQ5 and DCV induces various degrees of DDR, including activation of ATM, Chk2 and p53, which may have significant consequences on regulatory cell cycle pathways and apoptosis.

Keywords

ATM activation; histone H2AX phosphorylation; gammaH2AX; Chk2 activation; Ser15 p53 phosphorylation; checkpoint; DRAQ5; Hoechst33342; DyeCycle Violet; SYTO17; laser scanning cytometry

Introduction

The biomarkers applied supravitally should have a minimal effect on structure, function and survival of the interrogated cell. This is of special importance in studies that involve sorting cells with desired features for evaluation of their functional properties or further cloning and propagation as it is in the case of stem cells. However, most fluorochromes used as supravital cytometric probes affect the studied cells by interacting with different cell

Corresponding author: Dr. Z. Darzynkiewicz Brander Cancer Research Institute at NYMC Department of Pathology, BSB 438 Valhalla, NY 10595 Tel: 914-594-3780 Fax: 914-594-3790 darzynk@nymc.edu.

constituents and perturbing normal growth characteristics. These undesirable effects are often neglected by the investigators and the probes, marked by vendors as “supravital” or “probes of live cells” are being used without much scrutiny regarding their effects on the live cell.

The present study was designed to assess potential DNA damage induced by fluorescent probes frequently used to supravitally stain cellular nucleic acids. Specifically, we have measured the induction of ATM activation through its phosphorylation on Ser 1981, histone H2AX phosphorylation on Ser 139, activation of Chk2 protein kinase through its phosphorylation on Thr 68 and phosphorylation of p53 on Ser 15 in human pulmonary adenocarcinoma A549 cells treated with the supravital probes. All four phosphorylation events are considered to be reporters of the DNA damage response (DDR)(1⁻5). In our prior studies we have used phospho-specific Abs to detect these phosphorylation events in cells exposed to various genotoxic agents such as DNA topoisomerase inhibitors (6,7), tobacco smoke derived- (8) and acridine- mutagens (9) as well as exogenous and endogenous oxidants (10⁻12). We presently assessed DDR to the DNA minor grove ligand with a preference to A+T rich regions *bis*-benzimide Hoechst 33342 (Ho 42) (14), the DNA intercalating agent of the anthraquinone family DRAQ5 (13), the DNA binding probe Vybrant® DyeCycle Violet (DCV) (15), and the DNA/RNA ligand, the red permeant cyanine fluorochrome SYTO 17 frequently used to detect apoptosis (16,17). Towards this end, we exposed A549 cells to these probes at concentrations that are commonly used to supravitally examine cells, for short (up to 2 h) and prolonged (18 h) time intervals. The induction of ATM, H2AX, Chk2 and p53 phosphorylation was assessed immunocytochemically using the respective phospho-specific Abs and the cellular immunofluorescence was measured concurrent with DNA content by multiparameter laser scanning cytometry (LSC; iCys, refs.18,19). The bivariate analysis of immunofluorescence *versus* cellular DNA content measurements made it possible to correlate the DNA damage response with the cell cycle phase.

Materials and Methods

Cells, cell treatment

A549 cells, obtained from American Type Culture Collection (ATCC; Manassas, VA), were grown in Ham's F-12K Nutrient Mixture (Mediatech, Inc., Manassas, VA) supplemented with 10% fetal bovine serum, 100 units/ml penicillin, 100 μg/ml streptomycin and 2 mM L-glutamine (GIBCO/BRL; Grand Island, NY) in 25 ml FALCON flasks (Becton Dickinson Co., Franklin Lakes, NJ) at 37.5 °C in an atmosphere of 95 % air and 5% CO_2. The cells were maintained in exponential and asynchronous growth by repeated trypsinization and re-seeding prior to the culture reaching confluency. The cells were then trypsinized and seeded at low density (about 5×10^4 cells per chamber) in 2-chambered Falcon CultureSlides (Beckton Dickinson). Twenty four hours after seeding the cultures were treated with one of the probes: Ho 42 (Invitrogen/Molecular Probes, Eugene, OR), DRAQ (Axxora, LLC, San Diego, CA), DCV (Invitrogen/Molecular Probes) or SYTO 17 (Invitrogen/Molecular Probes). The time of treatment and concentrations of the respective probes are listed under Results and legends to figures.

Detection of histone H2AX phosphorylation on Ser139, ATM on Ser 1981, Chk2 on Thr 68 and p53 on Ser 15

Following incubations with the probes, the cells on slides were rinsed with PBS and then fixed with 1% methanol-free formaldehyde (Polysciences, Inc., Warrington, PA) in PBS for 15 min on ice followed by suspension in 70% ethanol where they were stored at −20° C for 2–24 h. The fixed cells were then washed twice in PBS and treated on slides with 0.1%

Triton X-100 (Sigma) in PBS for 15 min, and then in a 1% (w/v) solution of bovine serum albumin (BSA; Sigma) in PBS for 30 min to suppress nonspecific antibody (Ab) binding. The cells were then incubated in a 100 μl volume of 1% BSA containing 1:200 dilution of phospho-specific (Ser 139) H2AX mouse monoclonal antibody (Ab) (Biolegend, San Diego, CA) or 1:100 dilution of phospho-specific (Ser-1981) ATM mouse monoclonal Ab (Cell Signaling, Danvers, MA), or 1:100 diluted phospho-specific (Thr 68) Chk2 rabbit polyclonal Ab or 1:100 diluted phospho-specific (Ser 15) p53 rabbit polyclonal Ab (Cell Signaling) for 1.5 h at room temperature or overnight at 4 °C. The secondary fluorochrome-tagged Abs were chosen to have minimal spectral overlap with the supravital probes; thus the green fluorescing (Alexa Fluor 488) tagged Ab (Invitrogen/Molecular Probes, at 1;100 dilution) was used in the case of Hoechst 33342, DRAQ5, DCV, or SYTO 17 treated cells. In some experiments the far red emitting Alexa Fluor 633 Ab (Invitrogen/Molecular Probes, at 1:100 dilution) was also used for the cells treated with DCV. It should be noted, however, that fluorescence of the supravitally applied probes was markedly depressed after cell permeabilization and fixation that involved 70% ethanol, which additionally helped to prevent the interference of these probes with the emission of Alexa Fluor 488 or 633 tagged Abs. Prior to measurement by LSC, the cells were counterstained with 2.8 μg/ml 4,6-diamidino-2-phenylindole (DAPI; Sigma) in PBS for 15 min. Other details of cell incubations with the primary and secondary Ab were presented before (7¯11،20).

Measurement of cell fluorescence by LSC

Cellular green or far red IF representing binding of the respective phospho-specific Abs and the blue emission of DAPI stained DNA was measured using an LSC (iCys; CompuCyte, Cambridge, MA) utilizing standard filter settings; fluorescence was excited with 488-nm argon, helium-neon (633 nm) and violet (405 nm) lasers. The intensities of maximal pixel and integrated fluorescence were measured and recorded for each cell. At least 3,000 cells were measured per sample. Gating analysis was carried out to obtain mean values (± SE) of $p53Ser15^P$ for G_1 (DNA Index; DI = 0.9 –1.1), S (DI = 1.2 – 1.8) and G_2M (DI = 1.9 – 2.1) cell populations in each experiment. The standard deviation was estimated based on Poisson distribution of cell populations. Each experiment was run at least in triplicate, some experiments were additionally repeated. The inter-sample variation in the triplicates did not exceed the value of three standard deviations of individual samples. Other details are given in figure legends.

Results

Short term incubations with the probes

The first set of results pertains to short duration (up to 2 h) treatment of cells with individual probes (Figs.1–5). Exposure of cells to Ho 42 at 0.1 μM concentration led to a modest decrease in expression of γH2AX, seen predominantly in S- and G_2M phase- cells (Fig. 1). After treatment for 2 h the mean γH2AX IF of G_2M-cells was decreased by about 40% respective to control. A similar degree of decrease in γH2AX IF was observed in cells exposed to 1.0 or 2.0 μM Ho 42 for up to 2 h (not shown). Unlike the decline in γH2AX, an increase in ATM-$S1981^P$ IF was seen in cells treated with Ho 42 (Fig. 2). In the data presented in this figure, ATM-$S1981^P$ IF was recorded either as an integrated value (left panels) or as maximal pixel (middle panels). While the integrated value represents total ATM-$S1981^P$ IF intensity per cell the maximal pixel reports its highly localized intensity at the centrosomes/centrioles, reflecting activation of ATM in these organelles of mitotic and post-mitotic G_1 cells, as described before (10). Treatment with Ho 42 for 1 or 2 h led to about a 50% increase of integrated ATM-$S1981^P$ IF in G_2M cells and to a lesser degree in G_1 and S-phase cells. There was no apparent effect of Ho 42 on the intensity of ATM-$S1981^P$ IF in centrosomes/centrioles, although fewer postmitotic G_1 cells with elevated

levels of ATM-S1981^P IF were apparent in the Ho 42 treated culture (Fig. 2). Exposure of cells to Ho 42 at higher concentrations (up to 2 μM) for 1 or 2 h essentially had no effect on Chk2-Thr68^P or p53-Ser15^P IF (data not shown).

Fig. 3 shows changes in γH2AX IF after exposure of the cells to DRAQ5. The initial, small increase in γH2AX IF seen in G_2/M cells treated with 2 μM DRAQ5 for 0.5 h was followed by a distinct decrease of γH2AX IF, seen in all phases of the cell cycle, after 1 h and 2h of treatment with this probe. This attenuation of γH2AX IF was time and concentration dependent; exposure to10 μM DRAQ for only 0.5 h led to a dramatic decline in γH2AX IF. The changes in ATM-Ser1981 phosphorylation in cells treated with DRAQ5 are shown in Fig. 4. These changes were also time dependent. The initial increase in ATM-S1981^P IF occurring in all phases of the cell cycle was observed after cells exposure to the probe for 0.5 and 1 h but a decline, to the approximate level of ATM-S1981^P IF of untreated cells, was evident after 2 h. There was no significant evidence of change in the cell cycle distribution as reflected by the DNA content frequency histograms (Fig. 4, insets) except of some widening of the G_1 and G_2M peaks, likely due to a decline in stoichiometry of DNA staining with DAPI following exposure to DRAQ5. No significant changes in the level of phosphorylation of Chk2 on Thr68 or p53 on Ser15 were detected in the cells treated with 2 μM DRAQ5 for up to 3 h (not shown).

Treatment with DRAQ5, however, led to pronounced changes in chromatin structure (Fig. 5). The changes manifested themselves as a decrease in intensity of maximal pixel of DAPI fluorescence and an increase of nuclear area (number of pixels of DAPI fluorescence). The increase of nuclear area however was relatively minor. The decrease of the *ratio* of maximal pixel of DAPI fluorescence to nuclear area provided an even more distinct marker of these chromatin changes. This type of change is characteristic of chromatin decondensation and has been used as a marker discriminating cells differing in the extent of chromatin compaction such as mitotic *vs* interphase cells (21), lymphocytes *vs* granulocytes *vs* monocytes (22) or apoptotic *vs* non-apoptotic cells (23،24). In fact, whereas the presence of mitotic (M) and immediately postmitotic cells with condensed chromatin (pM) can easily be discerned in the control culture, no such cells were present in the DRAQ5 treated cultures (Fig. 5). No changes in chromatin that could be detected by analysis of maximal pixel of DAPI fluorescence were evident in cells treated for up to 2 h with other probes (not shown).

Exposure of A549 cells to DCV (5 μM) for 0.5, 1.0 or 2.0 h led to a decrease in expression of γH2AX, particularly in S and G_2M phase cells, and to a rather minor increase in phosphorylation of ATM (Supplemental data; Fig. 1). Even smaller changes in phosphorylation of Chk2-Thr68 and p53-Ser15 were seen in the cells treated with 5 μM DCV for up to 2 h (not shown).

Cell treatment with SYTO 17, at a concentration of 50 nM for up to 4 h had very minor effects on expression of γH2AX or ATM-S1981^P (Supplemental data, Fig. 2). Treatment with a higher SYTO 17 concentration (2.5 μM) for 2 h essentially had no effect on H2AX phosphorylation. However, it led to an increase in ATM-Ser1981^P IF by about 80% in all phases of the cell cycle (Supplemental data Fig. 3).

Prolonged (18 h) treatment with the probes

In the next set of experiments the cells were exposed to the individual probes for 18 h. Fig. 6 shows the DNA content frequency histograms of the untreated and treated cells, their nuclear area and maximal pixel of DAPI fluorescence. As it is evident that while exposure to 50 nM SYTO 17 had only minor effect on the cell cycle distribution, the DNA histogram of the cells treated with DCV reveals marked accumulation of cells in G_2M (28%) and in S (27%)compared to 23% and 17% seen in the untreated culture, respectively. In addition, the

percentage of G_2M cells was increased in Ho 42 (1 μM) and DRAQ5 (2 μM) treated cultures (27% and 28%, respectively, compared to 23% in control). However, a pronounced change in nuclear structure, manifested as a decrease in maximum pixel of DAPI fluorescence and consistent with chromatin decondensation was seen in cells growing in the presence of Ho 42 and DRAQ5. It should be noted that while DRAQ5 rapidly (within 1 h) induced this change in stainability with DAPI (Fig. 5), the decrease in intensity of maximal pixel of DAPI fluorescence in cells treated with Ho 42 was a late event, not seen during the initial 2 h of treatment. Visual inspection of over 200 images of cells treated with Ho 42 or DRAQ5 gated by LSC within the G_2M peak revealed the absence of mitotic cells.

The cell cycle progression in cultures treated with DCV was severely perturbed, marked by accumulation of cells in S (27%) and G_2M (38%). However, DNA stainability with DAPI (intensity of maximal pixel) was unchanged. Among the subpopulation of G_2M cells there were some mitotic cells, an indication that despite perturbation of cell cycle progression, cells were able to undergo mitosis.

Fig. 7 illustrates the changes in H2AX IF of cells treated for 18 h with each of the supravital probes. Exposure of cells to Ho 42 had a relatively modest effect, seen as a ~30% increase of mean values of γH2AX IF of G_1 and an ~40% decrease of G_2M cell subpopulations. Treatment with DRAQ5, however, led to a large increase in the extent of phosphorylation of H2AX. The increase was particularly pronounced in S phase cells, whose mean γH2AX IF was four-fold higher compared to untreated cell. The effect of DCV was rather modest, reflected by approximately 30% reduction of the mean value of γH2AX IF of G_2M cells. Treatment with SYTO 17 had no effect on γH2AX as the IF of the treated cells was essentially identical with that of the untreated ones.

Changes in the level of ATM phosphorylation in the cells treated with the probes are shown in Fig. 8. Treatment with Ho 42 led to a three- to four- fold rise in ATM-S1981^P IF in all phases of the cell cycle. Treatment with DRAQ5 resulted in an even greater increase in ATM phosphorylation, most pronounced (over five-fold) in S and G_2M phase cells. A nearly two-fold increase in ATM-S1981^P IF was observed in cells exposed to DCV. SYTO 17 exerted a minimal effect as the mean ATM-S1981^P IF of the treated cells was only about 15% higher that that of the untreated ones.

The pattern of Chk2 phosphorylation on Thr68 of cells treated with the probes resembled that of ATM phosphorylation (Fig. 9). Thus, the Ho 42 treated cells had two-to three fold higher Chk2-Thr68^P IF than the untreated cells. Also, the treatment with DRAQ5 led to several-fold increase in intensity of Chk2-Thr68^P IF, particularly in the S and G_2M phase cells. The cells treated with DCV had distinctly elevated Chk2-Thr68^P IF compared to control, while treatment with SYTO 17 essentially had no effect on the level of Chk2-Thr68P IF.

Fig. 10 presents the response of cells treated for 18 h with the probes in terms of p53 phosphorylation on Ser15. Strong induction of p53 phosphorylation was observed in the cells exposed to Ho 42. The mean p53-Ser15^P IF of the Ho 42 treated cells was increased in all phases of the cell cycle but the maximal (over four-fold) rise was in G_1 phase cells. There was large intercellular variation in the intensity of p53-Ser15^P IF, particularly among G_1 and G_2M cell subpopulations. In the case of DRAQ5 treated cells, the maximum response was seen in S-phase cells which had well over three-fold higher mean value of p53Ser15^P IF than the S-phase cells from untreated cultures. Also increased, but to a lesser degree (50–70%), was p53-Ser15^P IF of the cells treated with DCV. However p53-Ser15^P IF of the cells exposed to SYTO 17 was essentially unchanged compared to control.

Discussion

Exposure of A549 cells to Ho 42, DRAQ5 and DCV, within the range of concentrations with which these probes are being used supravitally, led to distinct changes characteristic of the DNA damage response. In addition, changes in chromatin structure that reflect altered chromatin condensation, as well as perturbations of cell cycle progression were detected. However, because of these changes in chromatin structure, which in the case of DRAQ5 were shown to be associated with dissociation of histone H1 from DNA followed by release of histone H2A from nucleosomal cores (25), it is difficult to interpret the observed decrease in γH2AX IF induced by this probe as due to a reduced level of H2AX phosphorylation. Dislocation of histones within the nucleosomal core may affect both phosphorylation of H2AX as well as accessibility of the phospho-epitope of γH2AX to the Ab. The summary of these observations and possible mechanisms are discussed for each of the probes studied.

Ho 42

Ho 42 is the most frequently used supravital biomarker of DNA (26). This fluorochrome is lipophilic, and unlike most other DNA probes, able to cross the intact cell membrane. Its application as a supravital probe is mainly in conjunction with the fluorescence-activated cell sorting to select cell residing in different phases of the cell cycle or with different DNA ploidy to assess their growth potential, metabolic properties, gene expression, drug sensitivity, *etc.* (27). Recently, however, the reduced binding of Ho 42 has become widely applied as a marker of hematopoietic pluripotent stem cells (28,29). Stem cells identified and sorted as the so-called “side population” following staining with Ho 42 are being used in numerous applications *in vitro* and *in vivo* including clinical trials (30). The attenuated binding of Ho 42 to DNA in the stem cells is primarily due to the highly active multidrug efflux pump which reduces the dye concentration within the cell. It should be noted, however, that although stem cells bind less Ho 42 than non-stem cells, the binding is still significant inasmuch as the intensity of Ho 42 in stem cells is within the range of 10–80% of the fluorescence of the non-stem cell population (28,29). The possible biological effects of Ho 42 on the sorted cells are often neglected. Yet it is known that Ho 42 is DNA topoisomerase I inhibitor, specifically interrupting the breakage/reunion of DNA and topoisomerase I by trapping reversible topoisomerase I cleavable complexes (31). It has also been reported that, under certain conditions, Ho 42 may be cytotoxic and mutagenic (32). Furthermore, Ho 42 and its close analog 33358 are known to sensitize cells to UV light; the energy transfer of the absorbed UV light from Hoechst to DNA results in crosslinking of histone proteins to DNA (33,34) and significant DNA photolysis when DNA is labeled with BrdU (35). Given the above, it was of interest to explore the potential effect of this probe in terms of induction of the DNA damage response.

Exposure of cells to 0.1 – 2.0 μM Ho 42 for up to 2 h led to a distinct decrease in the extent of γH2AX IF in S and G_2M cells (Fig. 1) and a modest (50%) increase in ATM phosphorylation in G_2M cells (Fig. 2). The effects were not concentration-dependent since similar drop of γH2AX and rise of ATM-Ser1981^P IF were seen over the concentration range of 0.1 to 2.0 μM. No significant changes in the level of Chk2 or p53 phosphorylation were seen and the DNA stainability with DAPI (maximal pixel vs nuclear) was unchanged during short-term treatment The observed decrease in γH2AX IF most likely reflects the Ho 42-induced change in chromatin structure due to its binding to the minor groove of DNA (13) that may restrict accessibility of the γH2AX epitope to the phospho-specific Ab. The alternative explanation, namely that Hoechst 33342 may lower the constitutive DNA damage caused by metabolically generated reactive oxidants *via* scavenging them (11,12,24), is less likely, because then a decrease, not an increase in ATM activation, would be observed. It is likely that the modest increase in ATM activation (Fig. 2) was triggered by binding of this probe to the minor grove of DNA followed by modification of DNA

structure. Unlike in the case of other DNA topoisomerase I or II inhibitors such as topotecan (7), mitoxantrone (7) or etoposide (6,36), the DNA damage response upon short treatment with Ho 42 was reflected by only a modest degree of ATM activation and not by a dramatic increase in H2AX or Chk2 phosphorylation.

Quite a different response to Ho 42 was apparent upon longer (18 h) exposure of cells to this probe. First, the increased proportion of cells in G_2M phase was evident on the DNA frequency histogram (Fig. 6). The visual analysis of cell images recorded by the LSC within the G_2M gate revealed a near total absence of mitotic cells. This observation would indicate that in cultures treated with 1 μM Ho 42, the progression through the cell cycle (particularly through G_2), was markedly perturbed and the cells did not undergo mitosis. Also, there was a distinct change in chromatin condensation reflected by the diminished intensity of maximal pixel of DAPI fluorescence (Fig. 6). The lack of cells with high maximal pixel DAPI fluorescence intensity confirmed the absence of mitotic and postmitotic cells. While there was still a somewhat reduced level of γH2AX IF compared to control (Fig. 7), the cells showed a several–fold increased level of activation of ATM (Fig. 8) and of Chk2 (Fig. 9) and also phosphorylation of p53 (Fig. 10). All these changes were not cell cycle phase specific, being induced to a comparable level in G_1, S and G_2M cells. Thus, the DNA damage response to Ho 42 was quite unique since it involved activation of ATM and Chk2 as well as p53 phosphorylation on Ser15, with no evidence of H2AX phosphorylation.

It should be noted that uptake of Ho 42 is temperature–dependent and minimal uptake is observed below 16 °C (37). As a supravital probe, however, Ho 42 is typically used at 37 °C, and the present observations on Ho 42-induced DDR pertain to the latter temperature at which the fluorochrome easily penetrates live cells.

DRAQ5

DRAQ5 was developed as a supravital stoichiometric DNA fluorochrome to be used to assess the cell cycle distribution or DNA ploidy of live cells (14). Unlike Ho 42 DRAQ5 can be excited at long wavelength (14,38) which markedly extends its applications. However DRAQ5 belongs to the class of the DNA intercalating agents of the anthraquinone family, very close in structure to the well characterized anticancer drug mitoxantrone [(1,4-dihydroxy-5,8-bis ((2-((2-hydroxyethyl)amino) ethyl)amino) anthraquinone], often abbreviated DHAQ (39). Mitoxantrone binds to DNA by intercalation, causes *in situ* condensation of nucleic acids and is a DNA topoisomerase II inhibitor (40). Its strong cytostatic (G_2 arrest) and cytotoxic properties provided the basis for its application as an effective drug in the treatment of acute leukemias. As mentioned, mitoxantrone induces a strong DNA damage response in terms of H2AX phosphorylation, and ATM and Chk2 activation (7,41). Given the similarity in molecular structure between DRAQ5 and mitoxantrone it might be expected that DRAQ5 may also induce damage to DNA and be cytostatic and cytotoxic. As mentioned, chromatin changes marked by dissociation of histone H1 from DNA, followed by release of histone H2B from nucleosome core particles occurs shortly after exposure of HeLa cells to DRAQ5 (25).

In the present study, we observed remarkable differences in the response of A549 cells to DRAQ5 depending on the length of treatment. A distinct decrease in γH2AX IF, which was DRAQ5 concentration-dependent, was seem during the initial 2 h of cell exposure (Fig. 3). Activation of ATM was apparent in cells treated with DRAQ5 for 0.5 and 1.0 h but not after 2 h (Fig. 4). However, there was no evidence of Chk2 activation or p53 phosphorylation at that time. On the other hand, the change in chromatin structure manifested as a marked decrease in intensity of maximal pixel of DAPI fluorescence and modest increase in the nuclear area, was seen within 1 h of administration of DRAQ5 (Fig. 5).

Exposure of cells to DRAQ5 for 18 h led to pronounced effects consistent with the induction of DNA damage response, a change in chromatin structure and the perturbation of cell cycle progression. The DNA damage response manifested itself by H2AX phosphorylation, ATM and Chk2 activation and phosphorylation of p53 on Ser15. Such changes are typical following induction of double-strand DNA breaks (DSB). Unlike Ho 42, the DRAQ5 induced DNA damage response was cell cycle phase specific, affecting primarily S phase cells. However, as with Ho 42, the change in chromatin structure was reflected by the reduced intensity of maximal pixel of DAPI fluorescence (Fig. 6). The lack of cells with high maximal pixel DAPI fluorescence typical of mitotic and postmitotic cells, the absence of mitotic cells in the images of cells gated within the G_2M peak and the increase in the proportion of G_2M cells in the DNA frequency histograms indicated perturbed progression of cells through all phases of the cell cycle but predominantly through G_2. This would be consistent with the observed Chk2 activation (Fig. 9), which by targeting Cdc25 protein phosphatases (primarily Cdc25C), halts cell cycle progression at the entrance to mitosis (42). The selective response of S phase cells to DRAQ5 may indicate that the mechanism of induction of DSB may involve collision of the replication forks with the primary lesions (“cleavable complexes”) caused by DRAQ5 such as is the case with other DNA topoisomerase I or II inhibitors (43،44).

As in our prior studies (25), we also analyzed confocal images of cells treated with DRAQ5 for 18 h. The HeLa cells having GFP-tagged histones treated with DRAQ5 for 18 h revealed a striking dependence of adverse effects on DRAQ5 concentration. While a treatment with 1 μM resulted in a population of cells showing only minor morphological changes and demonstrating intact plasma membrane (by the fluorescein-diacetate assay), cells treated with 2 μM DRAQ5 had irregular contours and aggregated chromatin, often in proximity of the nuclear envelope. In many cells, the integrity of the plasma membrane was compromised (data not shown). The morphological changes seen at high spatial resolution in HeLa cells expressing GFP-tagged histones are consistent with the previously described chromatin aggregation caused by DRAQ5 (25), followed by a complete loss of nuclear organization and subsequent gradual loss of cell functions.

DCV and SYTO 17

DCV is a convenient fluorochrome that unlike Ho 42 does not require UV excitation but can be excited with violet lasers. It offers certain advantages over Ho 42 as a “side population” marker for sorting stem cells (15،45،46). DCV together with two related dyes such as Vybrant DyeCycle Green (DCG) and Vybrant DyeCycle Orange (DCO) can also be used to assess the cell cycle distribution of live cells. This straightforward method has been advertised as a convenient enhancement for the multiparameter analysis of apoptosis. In our previous work we showed, however, that Vybrant DyeCycle Orange (DCO) causes profound cytotoxic effects on U937 and HL-60 cells that render long-term experiments unfeasible (47). The most prominent effect of treatment of A549 cells with DCV was suppression of cell cycle progression through G_2M and S (Fig. 6). Exposure to DCV also led to an increase in the level of activated ATM and Chk2 as well as of phosphorylated p53. These effects, however, were distinctly less pronounced compared to the effects induced by Ho 42 or DRAQ5.

Recently, a novel group of substituted unsymmetrical cyanine SYTO probes has become commercially available (48). The SYTO superfamily consists of four subfamilies spanning a broad range of visible excitation and emission spectra including blue, green, orange and red fluorescent probes (47، 48). Derived from thiazole orange, all SYTOs display low intrinsic fluorescence, with strong enhancement upon binding to DNA and/or RNA. Unlike Hoechst 33342, DRAQ5 or Vybrant DyeCycle fluorochromes none of the SYTOs can be considered as a selective DNA marker. As a result no stoichiometric incorporation is observed upon cell

entry of SYTOs (47). Following rapid entry into the cytoplasm, SYTO probes display nuclear or diffuse-cytoplasmic staining patterns (16, 17, 47). Although the resolution in localizing the dye is as yet poorly defined, suggestions have been made that it may reflect (i) gradient dependent dye uptake by mitochondria or other organelles like ER or Golgi or (ii) changes in chromatin condensation (17, 47). Cell permeability and broad selection of excitation/emission spectra has recently driven implementation of SYTO dyes in many polychromatic protocols with the detection of apoptosis being one of the most prominent applications (16,17,47,48).

In our current work, SYTO 17 at a concentration of 50 nM had no discernable effect on any of the measured parameters either after short-term (1–4 h) or after 18 h, treatment. However, exposure of cells to 2.5 μM SYTO 17, a concentration higher than is commonly used (16,17), induced some activation of ATM but had no effect on H2AX phosphorylation (Supplemental data Fig. 3). Therefore, SYTO 17 compared with Ho 42, DRAQ5 and DCV, had the least effect in terms of induction of the DNA damage response. These results support our earlier studies on non-toxic properties of green, orange and red fluorescent SYTO dyes (47). Recent studies also showed that, in contrast to DRAQ5, no histone detachment follows incorporation of SYTO 17 into nuclear DNA (25). Moreover, even at elevated doses, SYTO 17 causes only insignificantly low chromatin aggregation (25). It is also noteworthy that good intracellular retention of many SYTO molecules enables straightforward tracing of pre-labeled cell subpopulations for extended periods of time (47). Therefore, the lack of any adverse effects on cellular physiology strongly favors SYTO probes in applications requiring live-cell labeling (47).

Conclusions

Ho 42, DRAQ5 and DCV, to varying degrees, induced phosphorylation of proteins known to be responders to DNA damage. Phosphorylation of H2AX concurrent with activation of ATM, considered to be a reporter of induction of DSBs (2–5,49,50) were seen in cells treated with Ho 42 (in all phases of the cell cycle) and with DRAQ5 (predominantly in S-phase cells). Repair of DSBs is error prone resulting in deletion of base pairs and other defects that can cause translocations and chromosomal instability (51,52). ATM, Chk2 and p53 are key players in regulation of cell cycle progression and modulating apoptotic response. Their activation induced by the probes investigated in this study may have significant consequences on these regulatory pathways.

Supplementary Material

Refer to Web version on PubMed Central for supplementary material.

Acknowledgments

Supported by NCI; Grant number CA 28704. We thank Dr. Krzysztof Wojcik for help with confocal microscopy testing of the long-term effects of fluorescence probes.

Grant sponsor: NCI; Grant number CA 28704

References

1. Rogakou EP, Pilch DR, Orr AH, Ivanova VS, Bonner WM. DNA double-stranded breaks induce histone H2AX phosphorylation on serine 139. J Biol Chem. 1998; 273:5858–5868. [PubMed: 9488723]
2. Burma S, Chen BP, Murphy M, Kurimasa A, Chen DJ. ATM phosphorylates histone H2AX in response to DNA double-strand breaks. J Biol Chem. 2001; 276:42462–42467. [PubMed: 11571274]

3. Lavin MF, Kozlov S. ATM activation and DNA damage response. Cell Cycle. 2007; 6:931–942. [PubMed: 17457059]
4. Bartkova J, Bakkenist CJ, Rajpert-De Meyts E, Skakkebaek NE, Sehested M, Lukas J, Kastan MB, Bartek J. ATM activation in normal human tissues and testicular cancer. Cell Cycle. 2005; 4:838–845. [PubMed: 15846060]
5. Kinner A, Wu W, Staudt C, Iliakis G. γ-H2AX in recognition and signaling of DNA double-strand breaks in the context of chromatin. Nucleic Acids Res. 2008; 36:5678–5694. [PubMed: 18772227]
6. Tanaka T, Halicka HD, Traganos F, Seiter K, Darzynkiewicz Z. Induction of ATM activation, histone H2AX phosphorylation and apoptosis by etoposide: relation to the cell cycle phase. Cell Cycle. 2007; 6:371–376. [PubMed: 17297310]
7. Zhao H, Traganos F, Darzynkiewicz Z. Kinetics of histone H2AX phosphorylation and Chk2 activation in A549 cells treated with topotecan and mitoxantrone in relation to the cell cycle phase. Cytometry Part A. 2008; 73A:480–489.
8. Tanaka T, Huang X, Jorgensen E, Gietl E, Traganos F, Darzynkiewicz Z, Albino AP. ATM activation accompanies histone H2AX phosphorylation in A549 cells upon exposure to tobacco smoke. BMC Cell Biol. 2007; 8:26. Epub June 26. [PubMed: 17594478]
9. Pietrzak M, Halicka HD, Wieczorek Z, Wieczorek J, Darzynkiewicz Z. Attenuation of acridine mutagen ICR 191-DNA interactions and DNA damage by the mutagen interceptor chlorophyllin. Biophys J. 2008; 135:69–75.
10. Zhao H, Traganos F, Albino AP, Darzynkiewicz Z. Oxidative stress induces cell cycle-dependent Mre11 recruitment, ATM and Chk2 activation and histone H2AX phosphorylation. Cell Cycle. 2008; 7:1490–1495. [PubMed: 18418078]
11. Zhao H, Tanaka T, Halicka HD, Traganos F, Zarebski M, Dobrucki J, Darzynkiewicz Z. Cytometric assessment of DNA damage by exogenous and endogenous oxidants reports the aging-related processes. Cytometry Part A. 2007; 71A:905–914.
12. Tanaka T, Halicka HD, Huang X, Traganos F, Darzynkiewicz Z. Constitutive histone H2AX phosphorylation and ATM activation, the reporters of DNA damage by endogenous oxidants. Cell Cycle. 2006; 5:1940–1945. [PubMed: 16940754]
13. Chen AY, Yu C, Gatto B, Liu LF. DNA minor grove-binding ligands: a different class of mammalian DNA topoisomerase inhibitors. Proc Natl Acad Sci USA. 1993; 90:8131–8135. [PubMed: 7690143]
14. Smith PJ, Blunt N, Wiltshire M, Hoy T, Teesdale-Spittle P, Craven MR, Watson JV, Amos WB, Errington RJ, Patterson LH. Characteristics of a novel deep red/infrared fluorescent cell permeant DNA probe, DRAQ5, in intact human cells analyzed by flow cytometry and multiphoton microscopy. Cytometry. 2000; 40:280–291. [PubMed: 10918279]
15. Telford WG, Bradford J, Godfrey W, Robey RW, Bates SE. Side population analysis using a violet-excited cell permeable DNA binding dye. Stem Cells. 2007; 25:1029–1036. [PubMed: 17185610]
16. Wlodkowic D, Skommer J, Hillier C, Darzynkiewicz Z. Multiparameter detection of apoptosis using red-excitable SYTO probes. Cytometry Part A. 2008; 73A:563–569.
17. Wlodkowic D, Skommer J, Pelkonen J. Towards an understanding of apoptosis detection by SYTO dyes. Cytometry Part A. 2007; 71A:61–72.
18. Pozarowski P, Holden E, Darzynkiewicz Z. Laser scanning cytometry: Principles and applications. Meth Molec Biol. 2006; 319:165–192.
19. Darzynkiewicz Z, Bedner E, Gorczyca W, Melamed MR. Laser scanning cytometry. A new instrumentation with many applications. Exp Cell Res. 1999; 249:1–12. [PubMed: 10328948]
20. Zhao H, Traganos F, Darzynkiewicz Z. Phosphorylation of p53 on *Ser*15 during cell cycle caused by Topo I and Topo II inhibitors in relation to ATM and Chk2 activation. Cell Cycle. 2008; 7:3048–3055. [PubMed: 18802408]
21. Luther E, Kamentsky LA. Resolution of mitotic cells using laser scanning cytometry. Cytometry. 1996; 29:272–278. [PubMed: 8900469]
22. Bedner E, Burfeind P, Gorczyca W, Melamed MR, Darzynkiewicz Z. Laser scanning cytometry distinguishes lymphocytes, monocytes and granulocytes by differences in their chromatin structure. Cytometry. 1997; 29:191–196. [PubMed: 9389435]

23. Bedner E, Li X, Gorczyca W, Melamed MR, Darzynkiewicz Z. Analysis of apoptosis by laser scanning cytometry. Cytometry. 1999; 35:181–195. [PubMed: 10082299]
24. Huang X, Tanaka T, Kurose A, Traganos F, Darzynkiewicz, Z. Constitutive histone H2AX phosphorylation on *Ser*-139 in cells untreated by genotoxic agents is cell-cycle phase specific and attenuated by scavenging reactive oxygen species. Int J Oncol. 2006; 29:495–501. [PubMed: 16820894]
25. Wojcik K, Dobrucki JW. Interaction of a DNA intercalator DRAQ5, and a minor groove binder SYTO17, with chromatin in live cells - influence on chromatin organization and histone-DNA interactions. Cytometry Part A. 2008; 73A:555–562.
26. Darzynkiewicz Z, Crissman HA, Jacobberger JW. Cytometry of the cell cycle. Cycling through history. Cytometry Part A. 2004; 58A:21–32.
27. Juan G, Hernando E, Cordon-Cardo C. Separation of live cells in different phases of the cell cycle for gene expression analysis. Cytometry. 2002; 49:170–175. [PubMed: 12454980]
28. Godell MA, Brose K, Paradis G, Conner AS, Mullican RC. Isolation and functional properties of murine hematopoietic stem cells that are replicating *in vivo*. J Exp Med. 1996; 183:1797–1806. [PubMed: 8666936]
29. Leemhuis T, Yoder MC, Grigsby S, Aguero B, Eder P, Srour EF. Isolation of primitive human bone marrow hematopoietic progenitor cells using Hoechst 33342 and Rhodamine 123. Exp Hematol. 1996; 24:1215–1224. [PubMed: 8765497]
30. Segers VFM, Lee RT. Stem-cell therapy for cardiac disease (Review). Nature. 2008; 451:937–943. [PubMed: 18288183]
31. Chen AY, Yu C, Bodley A, Peng LF, Liu LF. A new mammalian DNA topoisomerase I poison Hoechst 33342: Cytotoxicity and drug resistance in human cell cultures. Cancer Res. 1993; 53:1332–1337. [PubMed: 8383008]
32. Durand RE, Olive PL. Cytotoxicity, mutagenicity and DNA damage by Hoechst 33342. J Histochem Cytochem. 1982; 30:111–116. [PubMed: 7061816]
33. Davis SK, Bardeen CJ. Cross-linking of histone proteins to DNA by UV illumination of chromatin stained with Hoechst 33342. Photochem Photobiol. 2003; 77:675–679. [PubMed: 12870855]
34. Singh S, Dwarakanath BS, Mathew TL. DNA ligand Hoechst-33342 enhances UV induced cytotoxicity in human glioma cells. J Photochem Photobiol B. 2004; 77:45–54. [PubMed: 15542361]
35. Huang X, King M, Halicka DH, Traganos F, Okafuji M, Darzynkiewicz Z. HistoneH2AX phosphorylation induced by selective photolysis of BrdU-labeled DNA with UV light: relationship to cell cycle phase. Cytometry Part A. 2004; 62A:1–7.
36. Smart DJ, Halicka HD, Schmuck G, Traganos F, Darzynkiewicz Z, Williams GM. Assessment of DNA double-strand breaks and γH2AX induced by the topoisomerase II poisons etoposide and mitoxantrone. Mutat Res. 2008; 641:43–47. [PubMed: 18423498]
37. Szabo G Jr, Kiss A, Damjanovich A. Flow cytometric analysis of the uptake of Hoechst 33342 dye by human lymphocytes". Cytometry. 1981; 2:20–23. [PubMed: 6168456]
38. Martin RM, Leonhardt H, Cardoso MC. DNA labeling in living cells. Cytometry Part A. 2005; 67A:45–52.
39. Kapuscinski J, Darzynkiewicz, Z. Interactions of antitumor agents ametantrone and mitoxantrone (Novantrone) with double-stranded DNA. Biochem Pharmacol. 1985; 34:4203–4213. [PubMed: 4074383]
40. Kapuscinski J, Darzynkiewicz Z. Relationship between the pharmacological activity of antitumor drugs Ametantrone and Mitoxantrone (Novatrone) and their ability to condense nucleic acids. Proc Natl Acad Sci USA. 1986; 83:6302–6306. [PubMed: 3462696]
41. Huang X, Kurose A, Tanaka T, Traganos F, Dai W, Darzynkiewicz Z. Activation of ATM and histone H2AX phosphorylation induced by mitoxantrone but not by topotecan is prevented by the antioxidant N-acetyl-L-cysteine. Cancer Biol Ther. 2006; 5:959–964. [PubMed: 16760673]
42. Ahn J, Urist M, Prives C. The Chk2 protein kinase. DNA repair. 2004; 3:1039–1047. [PubMed: 15279791]
43. D'Arpa P, Beardmore C, Liu LF. Involvement of nucleic acid synthesis in cell killing mechanisms of topoisomerase poisons. Cancer Res. 1990; 50:6916–6924.

44. Del Bino G, Lassota P, Darzynkiewicz Z. The S-phase cytotoxicity of camptothecin. Exp Cell Res. 1991; 193:27–35. [PubMed: 1995300]
45. She JJ, Zhang PG, Wang ZM, Gan WM, Che XM. Identification of side population cells from bladder cancer cells by DyeCycle Violet staining. Cancer Biol Ther. 2008; 7:1663–1669. [PubMed: 18787416]
46. Mathew G, Timm EA Jr, Sotomayor P, Godoy A, Montecinos VP, Smith GJ, Huss WJ. ABCG2-mediated DyeCycle Violet efflux defined side population in benign and malignant prostate. Cell Cycle. 2009; 8:1–9. [PubMed: 19182532]
47. Wlodkowic D, Skommer J, Darzynkiewicz Z. SYTO probes in the cytometry of tumor cell death. Cytometry Part A. 2008; 73A:496–507.
48. Frey T. Nucleic acid dyes for detection of apoptosis in live cells. Cytometry. 1995; 21:265–274. [PubMed: 8582249]
49. Kitagawa R, Bakkenist CJ, McKinnon PJ, Kastan MB. Phosphorylation of SMC1 is a critical downstream event in the ATM-ANBS1-BRCA1 pathway. Genes Dev. 2004; 18:1423–1438. [PubMed: 15175241]
50. Kitagawa R, Kastan MB. The ATM-dependent DNA damage signaling pathway. Cold Spring Harb Symp Quant Biol. 2005; 70:99–109. [PubMed: 16869743]
51. Vilenchik MM, Knudson AG. Endogenous DNA double-strand breaks: Production, fidelity of repair, and induction of cancer. Proc Natl Acad Sci USA. 2003; 100:12871–12876. [PubMed: 14566050]
52. Jeggo PA, Lobrich M. Artemis links ATM to double strand end rejoining. Cell Cycle. 2005; 4:359–362. [PubMed: 15684609]

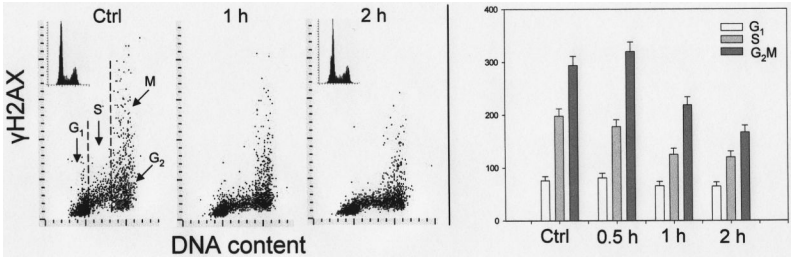

Fig. 1.

Changes in expression of γH2AX in A549 cells treated with Ho 42 in relation to the cell cycle phase.

The bivariate distributions (scatterplots) shown in left panels illustrate expression of γH2AX in untreated cells (Ctrl) or the cells exposed to Ho 42 at 0.1 μM concentration for 1 or 2 h in relation to cellular DNA content. DNA content histograms of the untreated and 2 h treated cells as presented in the insets. Based on differences in DNA content cells in G_1, S and G_2M phases of the cell cycle were gated (as shown) and mean values of γH2AX IF (+SD) of these cell populations are presented in the form of bar graphs (right panel).

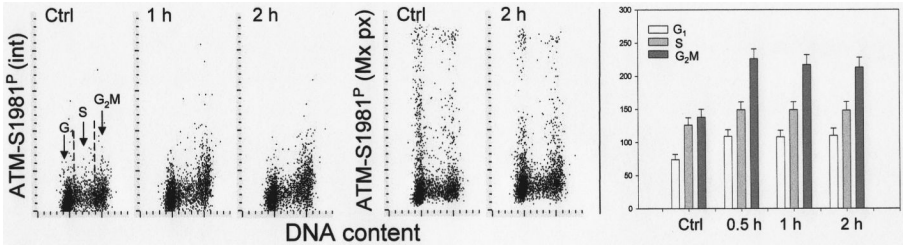

Fig. 2.

Changes in expression of ATM-S1981^P in A549 cells treated with Ho 42 in relation to the cell cycle phase.

The bivariate distributions reveal expression of ATM-S1981P recorded either as integrated value (int) or maximal pixel (Mx px) with respect to DNA content in untreated cells (Ctrl) or the cells exposed to Ho 42 at 0.1 μM concentration for 1 or 2 h in relation to cellular DNA content. Based on differences in DNA content cells in G_1, S and G_2M phases of the cell cycle were gated (as shown) and mean values of γH2AX IF (+SD) of these cell populations are presented in the form of bar graphs (right panel).

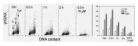

Fig. 3.

Changes in expression of γH2AX in A549 cells treated with DRAQ5 in relation to the cell cycle phase.

The bivariate distributions shown in left panels illustrate expression of γH2AX in the cells exposed to DRAQ5 at 2 μM concentration for 30 min, 1 or 2 h or to 10μM DRAQ5 for 30 min versus DNA content. The DNA content histograms of the untreated and 2 h-treated cells are shown in the respective insets. Based on differences in DNA content cells in G_1, S and G_2M phases of the cell cycle were gated as shown and mean values of γH2AX IF (+SD) of these cell populations are presented as bar graphs (right panel).

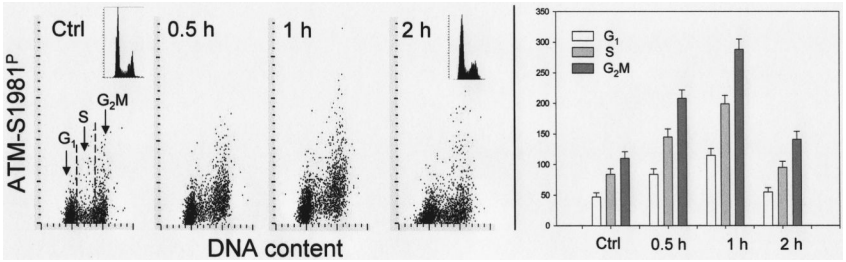

Fig. 4.

Changes in expression of ATM phosphorylated on Ser1981 in A549 cells treated with DRAQ5 in relation to the cell cycle phase.

The bivariate distributions show expression of ATM-S1981^P in the cells exposed to 2 μM DRAQ5 for 30 min, 1 h and 2 h with respect to their DNA content. The DNA content histograms of the untreated and 2 h-treated cells are shown in the respective insets. The bar graph illustrates the mean values of ATM-S1981^P immunofluorescence of cells in relation at different phases of the cell cycle.

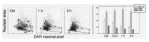

Fig. 5.

Effect of DRAQ5 on chromatin structure of A549 cells.

The cells were untreated (Ctrl) or treated with DRAQ5 at 2 μM concentration for 1 or 2 h, then fixed. The bivariate distributions (left panels) show the nuclear area (contoured on DAPI fluorescence) plotted against the maximal pixel intensity of DAPI fluorescence. The right panel shows bar graphs representing in mean values (+SD) of maximal pixel (Max pix), nuclear area (Area) and of ratio of maximal pixel to nuclear area (MP/Area) of all cells, untreated and treated with DRAQ5. To exclude doublets and debris the cells were gated as shown in individual panels by solid lines. The cells characterized by high intensity maximal pixel (in Ctrl) are either mitotic (M) or post-mitotic (pM), identified by their imaging. The decline in intensity of maximal pixel fluorescence of the DNA-associated fluorescence such as DAPI concurrent with some increase in nuclear area, as seen in DRAQ5 treated cells, is a characteristic feature of chromatin decondensation.

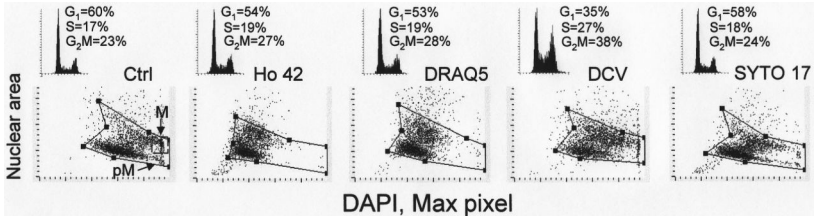

Fig. 6.

Cell cycle distribution and chromatin status (nuclear area vs maximal pixel of DAPI fluorescence) of A549 cells exposed in cultures to Ho 42 (1 μM), DRAQ5 (2 μM), DCV (5 μM) or SYTO 17 (50 nM) for 18 h.

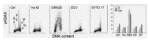

Fig. 7.

Effect of exposure of A549 cells to the studied probes for 18 h on H2AX phosphorylation. The bivariate (DNA content vs γH2AX IF) distributions of the untreated cells (Ctrl) and the cells treated in cultures with 1 μM Ho 42, 2 μM DRAQ5, 5 μM DCV and 50 nM SYTO 17 for 18 h. Subpopulations of G_1, S and G_2M cells were gated based on differences in cellular DNA content and their mean values of γH2AX IF (+SD) are presented as bar graphs (right panel).

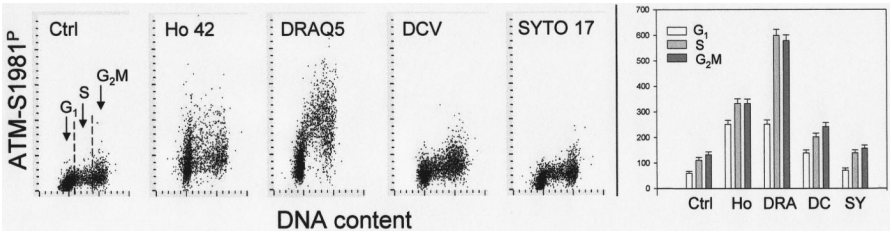

Fig. 8.

Effect of treatment of A549 cells with the studied probes for 18 h on phosphorylation of ATM on Ser 1981.

The bivariate (DNA content vs ATM-S1981^P) distributions of the untreated cells (Ctrl) and the cells treated in cultures with 1 μM Ho 42, 2 μM DRAQ5, 5 μM DCV and 50 nM SYTO 17 for 18 h. The mean values of ATM-S1981^P (+SD) of G_1, S and G_2M cells are presented as bar graphs (right panel; Ho-Hoechst 33342; DRA-DRAQ5; DC-DCV; SY-SYTO 17).

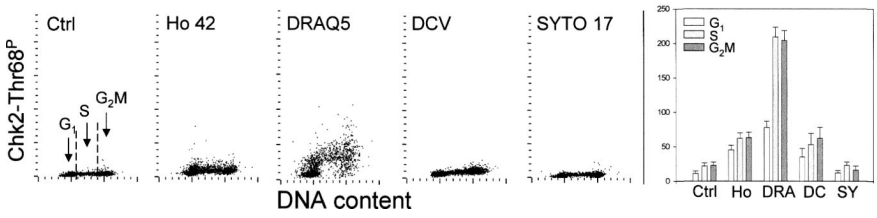

Fig. 9.

Effect of treatment of A549 cells with the studied probes for 18 h on Chk2 phosphorylation on Thr68.

The bivariate (DNA content vs Chk2-Thr68^P) distributions of the untreated cells (Ctrl) and the cells treated in cultures with 1 μM Ho 42, 2 μM DRAQ5, 5 μM DCV and 50 nM SYTO 17 for 18 h. The mean values of Chk2-Thr68^P (+SD) of G_1, S and G_2M cells are presented as bar graphs (right panel: Ho-Ho 42; DRA-DRAQ5; DC-DCV; SY-SYTO 17).

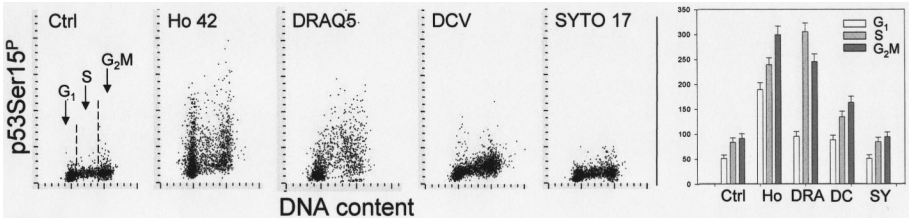

Fig. 10.

Phosphorylation of p53 on Ser 15 in A549 cells treated with the studied probes for 18 h. The bivariate (DNA content vs p53-S15^{P}) distributions of the untreated cells (Ctrl) and the cells treated in cultures with 1 μM Hoechst 33 42, 2 μM DRAQ5, 5 μM DCV and 50 nM SYTO 17 for 18 h. The mean values of p53-S15P (+SD) of G_1, S and G_2M cells are presented as bar graphs (right panel: Ho-Ho 42; DRA-DRAQ5; DC-DCV; SY-SYTO 17).